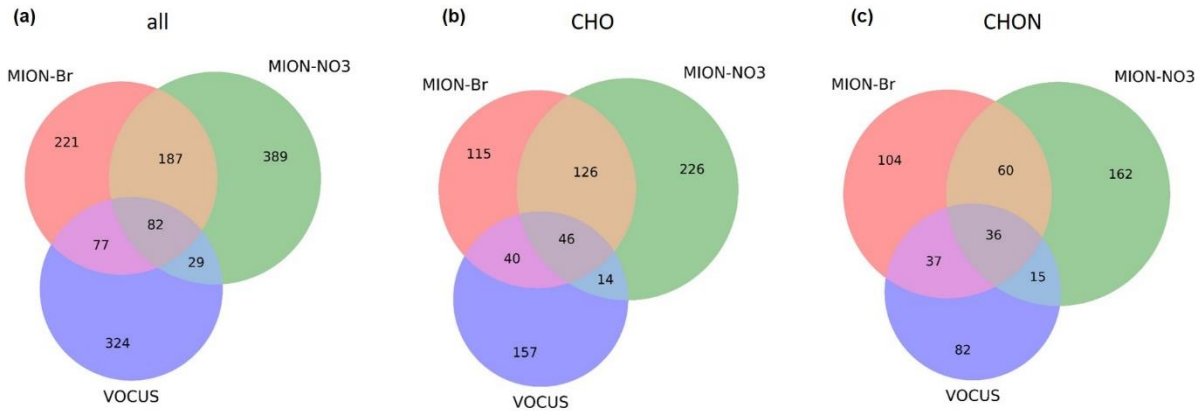

Figure S1. Overlaps of all organic compounds **(a)**, CHO compounds **(b)**, and CHON compounds **(c)** measured by Vocus, MION-Br, and MION-NO_3.

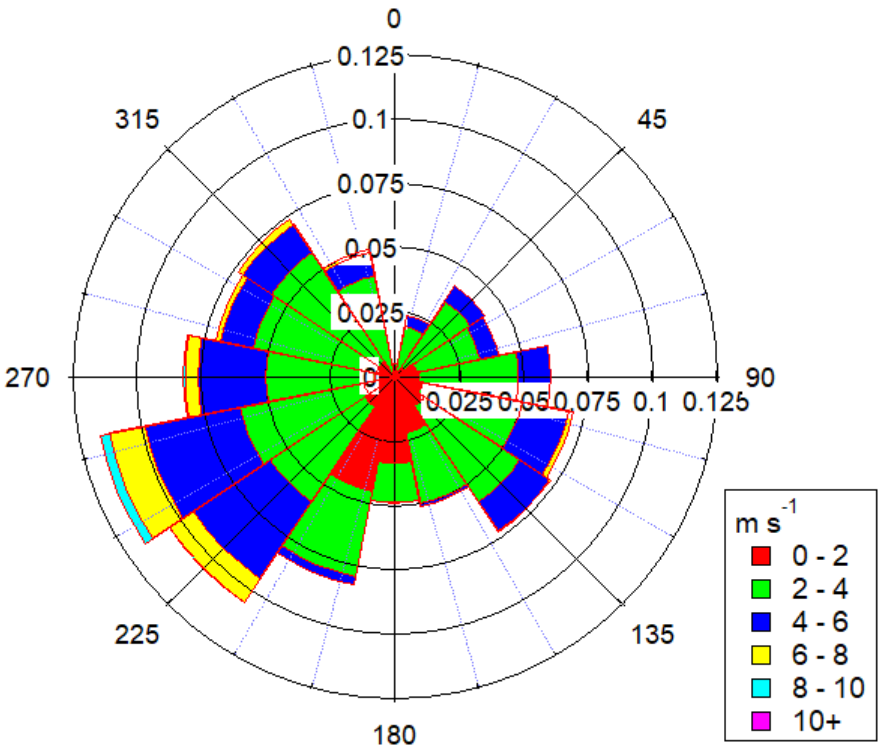

Figure S2. Wind speeds and directions during the measurement period.

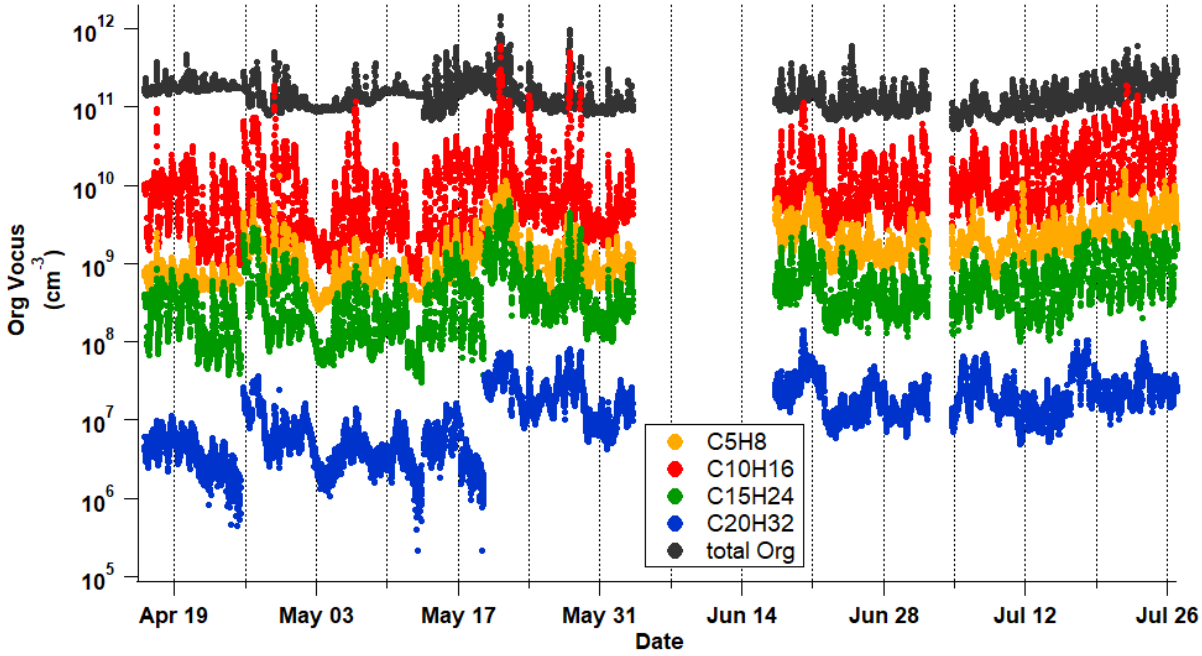

Figure S3. Time series of terpenes (isoprene, monoterpenes, sesquiterpenes, and diterpenes) and all organic compounds (for comparison, same as in Fig. 1f) measured by Vocus.

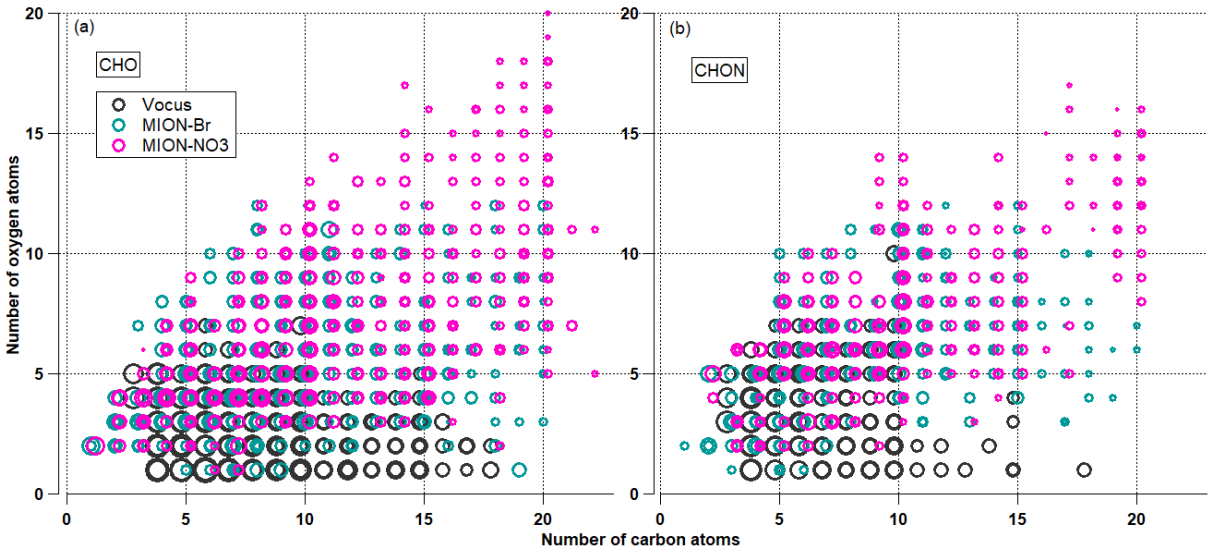

Figure S4. Distribution of CHO compounds **(a)** and CHON compounds **(b)** measured by Vocus, MION-Br, and MION-NO_3 as a function of number of oxygen atoms vs. number of carbon atoms. Markers were sized by the logarithm of their corresponding concentrations.

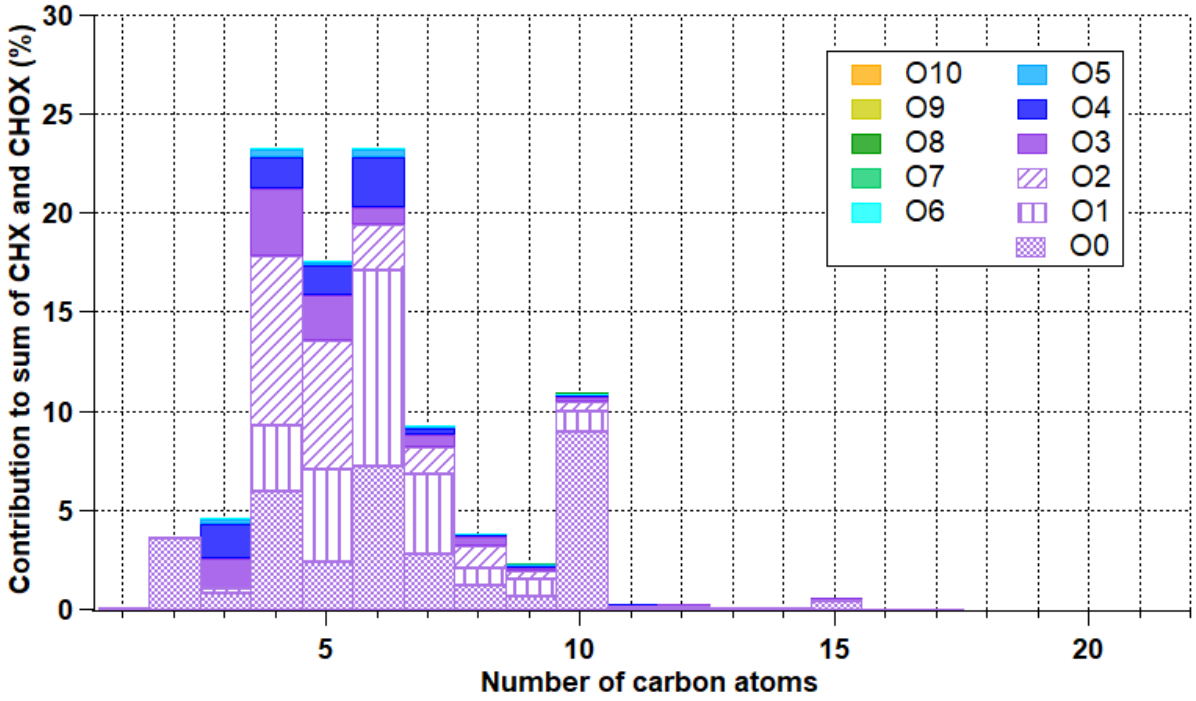

Figure S5. Contribution of organic compounds with different number of oxygen atoms to all organic compounds (including CHX compounds) as a function of the number of carbon atoms measured by Vocus.

Table S1. Sum contribution (%, average ± 1 standard deviation) of C_xH, C_xHO, and C_xHON groups (x = 5, 10, 15, and 20) to total CH, CHO and CHON compounds measured by different measurement techniques.

Compound group	Vocus	MION-Br	MION-NO_3
C_xH/CH	35.5 ± 11.3 %	-	-
C_xHO/CHO	27.3 ± 3.2 %	20.0 ± 4.4 %	26.8 ± 5.7 %
C_xHON/CHON	16.2 ± 2.3 %	34.9 ± 4.2 %	38.6 ± 4.5 %

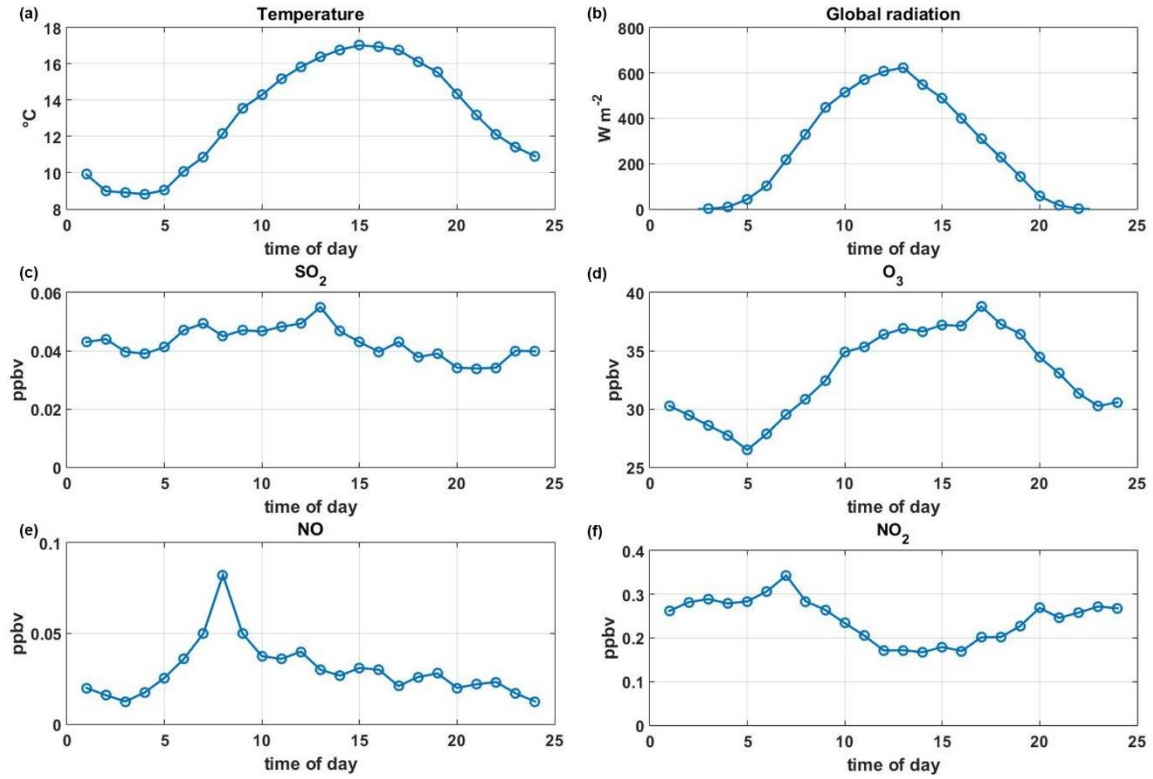

Figure S6. The median diurnal patterns of temperature **(a)**, global radiation **(b)**, mixing ratios of SO_2 **(c)**, O_3 **(d)**, NO **(e)**, and NO_2 **(f)** during the measurement period.

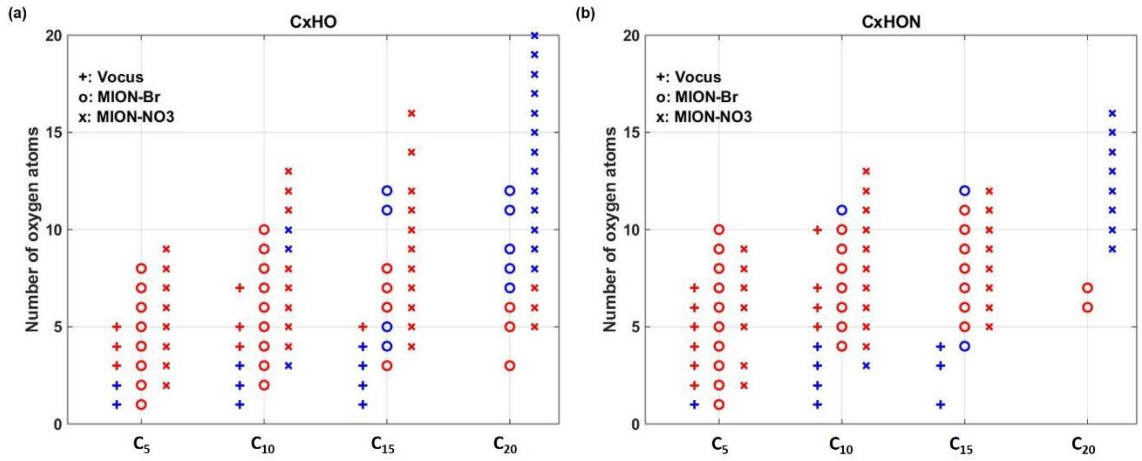

Figure S7. Comparison of the daytime (between 10:00 and 17:00) and nighttime (between 22:00 and 05:00) levels of C_xHO **(a)** and C_xHON **(b)** compounds (x = 5, 10, 15, 20) as a function of the number of oxygen atoms measured by Vocus (in pluses), MION-Br (in circles), and MION-NO_3 (in crosses). Compounds with higher signals during the daytime are colored in red and those with higher signals during the nighttime are colored in blue.

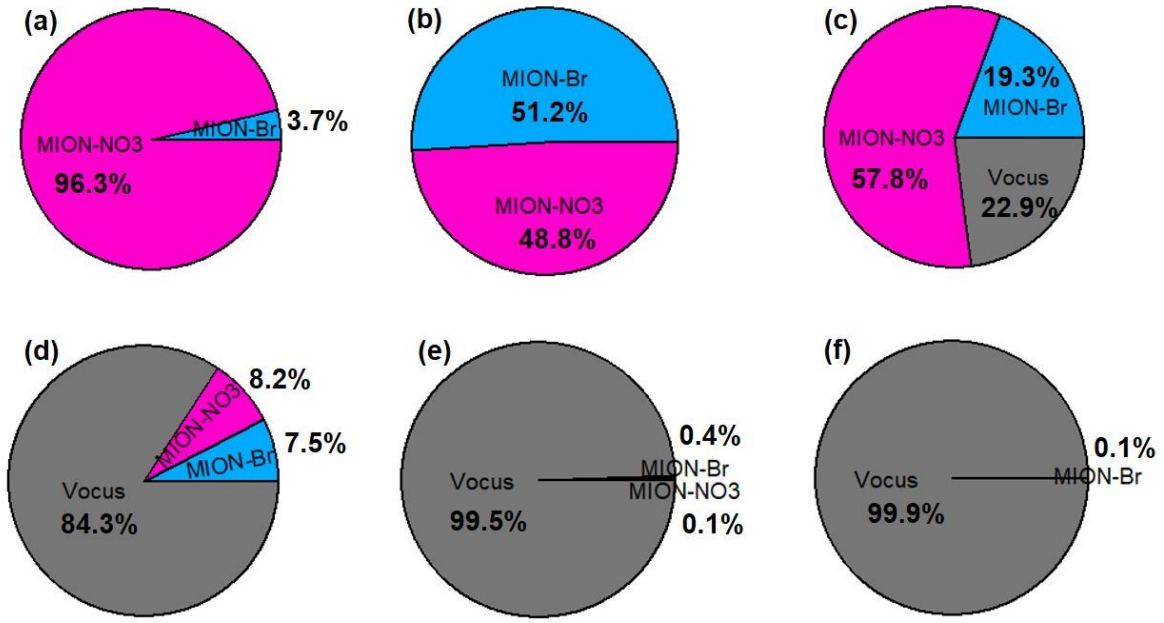

Figure S8. Fraction of ULVOC **(a)**, ELVOC **(b)**, LVOC **(c)**, SVOC **(d)**, IVOC **(e)**, and VOC **(f)** detected by Vocus, MION-Br, and MION-NO_3.

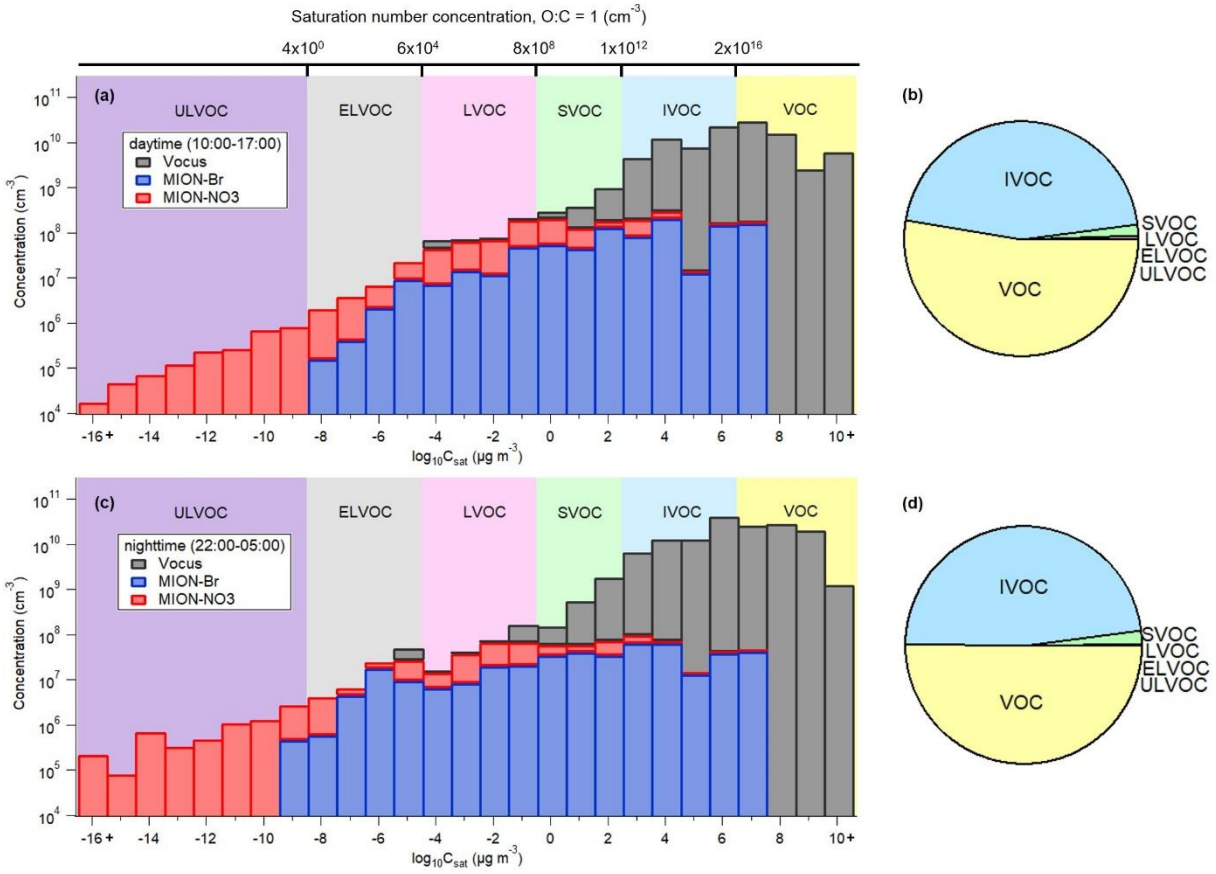

Figure S9. Stacked bar plots of combined volatility distribution for measured organic compounds parameterized with the approach of Li et al. (2016) during the daytime **(a)** and nighttime **(c)**; resulting pie charts for the contributions of VOC, IVOC, SVOC, LVOC, ELVOC, and ULVOC during the daytime **(b)** and nighttime **(d)**.

References

Li, Y., Pöschl, U., and Shiraiwa, M.: Molecular corridors and parameterizations of volatility in the chemical evolution of organic aerosols, Atmos Chem Phys, 16, 3327–3344, https://doi.org/10.5194/acp-16-3327-2016, 2016.